Chapter 6
Cognitive MAC Protocol with Transmission Tax: Probabilistic Analysis and Performance Improvements

Vojislav B. Mišić and Jelena Mišić

Abstract We investigate the performance of a cognitive personal area network (CPAN) in which spectrum sensing is linked to packet transmissions. Efficient CPAN operation may be achieved if each data transmission is taxed by requiring the transmitting node to participate in cooperative sensing for a prescribed time period. In this approach, each node is allowed to transmit a single packet in one transmission cycle, but must then 'pay' for it by spectrum sensing, which not only ensures fairness with respect to transmission but also distributes the sensing burden to all nodes. We describe a probabilistic model of the integrated system and evaluate its performance with respect to packet transmissions and spectrum sensing. We discuss two modifications that involve centralized and distributed selection of the channels to be sensed. We also propose an adaptive algorithm to determine the tax coefficient and show that it offers superior data transmission performance while not affecting the sensing accuracy.

6.1 Introduction

The cognitive communications paradigm (also known as opportunistic spectrum access, or OSA) allows efficient use of existing wireless spectrum opportunities [1, 2] in many wireless networks. In case of wireless personal area networks (PANs), opportunistic spectrum access may be combined with frequency hopping spread spectrum (FHSS) [3] to offer increased resilience to interference from primary users' activity. Unlike earlier FHSS technologies such as Bluetooth [4], the hopping sequence of a frequency-hopping cognitive personal area network (CPAN) should not only be random, but also dynamically adapted to primary users' activity patterns, which in turn necessitates accurate and timely sensing of all working channels in the chosen band. Fig. 6.1 schematically shows frequency hopping in a CPAN.

Efficient operation of a frequency-hopping OSA network is critically dependent on accurate and timely sensing of all working channels in the chosen band. Ideally, all channels should be sensed all the time [5], but in reality there is an error which is

V.B. Mišić (✉)
Department of Computer Science, Ryerson University, Toronto, ON M5B 2K3, Canada
e-mail: vmisic@scs.ryerson.ca

F.R. Yu (ed.), *Cognitive Radio Mobile Ad Hoc Networks*,
DOI 10.1007/978-1-4419-6172-3_6,

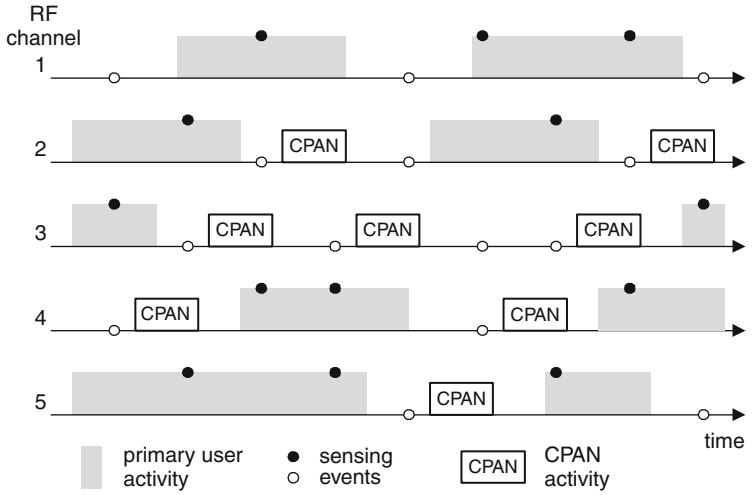

Fig. 6.1 Frequency hopping in a CPAN

caused by two factors. First, sensing is performed in discrete intervals, and changes in channel status (which can occur at any time) are not detected until the next sensing event [6]. Second, not all channels are sensed in every sensing cycle, and the delay in detecting the channel status may be longer than the sensing cycle.

However, if the CPAN coordinator is the only node to perform the sensing, sensing error may be unacceptably high [7] since each sensing takes a finite time, which limits the number of channels that can be sensed. This problem may be overcome by requiring that ordinary nodes in the CPAN help with sensing: this is commonly referred to as *cooperative sensing* [6]. The coordinator, then, coordinates the sensing process through scheduling sensing events, collecting the results, and combining them to form a coherent map of busy and idle channels [6, 8].

At the same time, CPAN nodes have data traffic to send to and receive from each other, which obviously interferes with sensing. As a result, a high-level balance must be struck between communication and sensing activities for each node, and a suitable protocol to schedule their individual activities must also be devised. It is the duty of the CPAN coordinator to ensure fairness among nodes, which means not only equal opportunities for transmission but also equal contribution to smooth operation of the CPAN through sensing. As transmission and sensing activities cannot be done at the same time, an effective balance between the two must be achieved and maintained, which necessitates a flexible transmission scheduling protocol.

In this chapter, we present one such protocol at the MAC level in which equal opportunity to transmit a single packet is given to all nodes through round robin scheduling. At the same time, nodes are required to 'pay' for transmissions by conducting sensing after transmission; this mechanism will be referred to as the 'transmission tax.' For each packet transmitted, the node has to perform spectrum

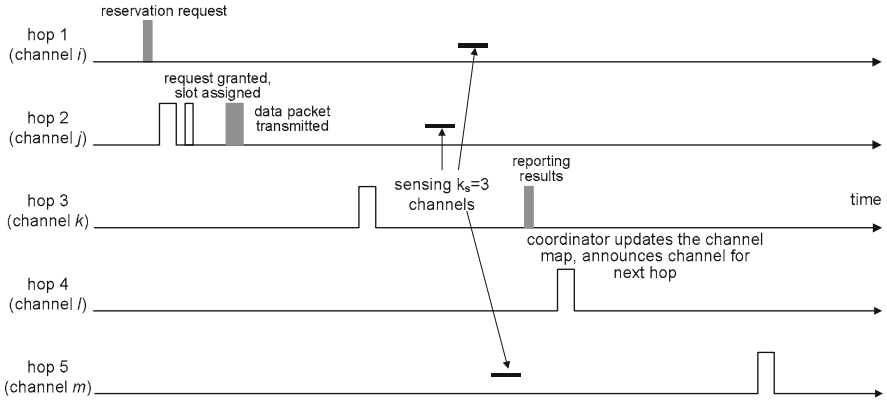

Fig. 6.2 CPAN operation: node activity for a single data packet to be transmitted

sensing on some k_s channels [9]. A schematic view of node activity related to a single packet to be transmitted is shown in Fig. 6.2. (For clarity, we have aligned the different channels from top to bottom, even though the actual channels may occur in any order, depending on the activity of primary sources.) In this manner, all nodes in the CPAN will be given equal opportunity to transmit data, but at the same time, all of them are expected to equally contribute to sensing, which reduces sensing errors and, thus, ensures smooth operation of the CPAN. The value of k_s is determined by the coordinator which monitors the CPAN traffic and maintains the channel map, with the goal of keeping the total sensing error below some pre-defined limit. Reception is not penalized, as will be seen below, and it does not affect the ratio of the number of transmitted packets to the sensing time. We then present a detailed probabilistic analysis of the integrated protocol and discuss its performance.

Several factors may affect the performance of the CPAN in this setting. Obviously, the tax rate will be the most important among them, as it limits the amount of time a node can spend in transmission, and its value has to be carefully chosen for the best tradeoff between transmission and sensing. The accuracy of sensing may be affected by the initial selection of channels to be sensed, and it may be done in a centralized fashion (i.e., by the coordinator) or it in a distributed fashion, locally by each node. We will investigate the performance of both approaches. Finally, we propose a simple adaptive algorithm for determining the tax rate so as to maintain a steady influx of sensing information.

The chapter is organized as follows: Section 6.2 gives more details about the operation of a frequency hopping cognitive personal area network, while Section 6.3 models the durations of transmission, sensing, and waiting times. Packet access delay is derived in Section 6.4. In Section 6.5 we present sensing model with control of sensing error. Section 6.6 presents the performance of the original protocol with respect to both data transmission and sensing. Modifications regarding the selection

of channels to be sensed, as well as their performance, are presented in Section 6.7. The adaptive tax protocol is described in Section 6.8, while Section 6.9 concludes the chapter and highlights some avenues for future research.

6.2 The Transmission Tax-Based Protocol

A CPAN piconet consists of a dedicated coordinator and a number of nodes. The coordinator is responsible for starting the piconet, admitting nodes to join the piconet, monitoring and controlling its operation, and for other administrative tasks. Time is partitioned into superframes of fixed size, similar to other recent communication technologies such as IEEE 802.15.3 [10]. Each superframe is marked by a beacon frame emitted by the coordinator; activities such as node association and disassociation, bandwidth allocation requests and announcements, sensing allocation and reporting, and actual data transfers take part in dedicated sub-frames within the superframe, as shown in Fig. 6.3.

Each superframe uses a different channel from the working channel set, and the hopping sequence is random as well as adaptive, in the sense that the next working channel is chosen in a pseudo-random manner from the set of channels which are currently free of primary source activity. The working frequency band consists of N channels, each of which is used by a distinct primary source which operates in an ON-OFF regime. The durations of active and inactive periods of these sources may be characterized with suitable probability distributions. For simplicity, we assume that all primary sources have the same mean durations of active and inactive periods and, consequently, the same value of the activity factor $p_{a,r}$.

When the node has data to transmit, it requests a suitable bandwidth allocation, expressed as a certain number of time slots, during the reservation sub-frame in hop 1. Each node can request transmission of at most one packet in a single request. The coordinator receives the requests and allocates time slots to nodes in a

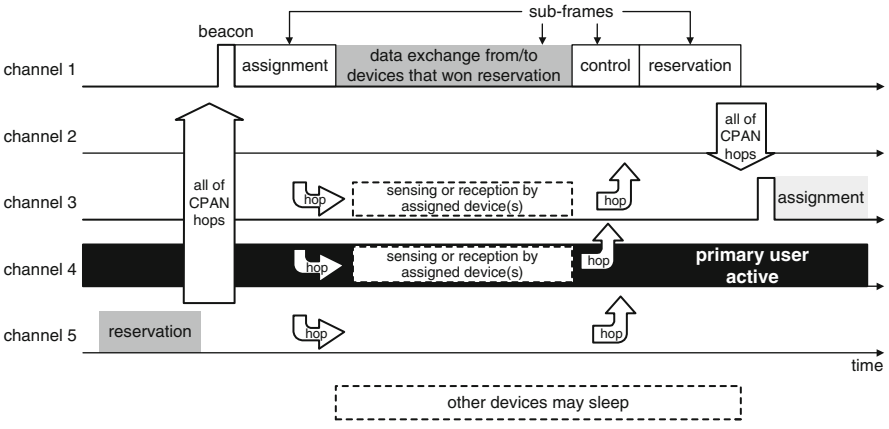

Fig. 6.3 Superframe format and node activities

round-robin fashion, as follows. All requests received during the reservation slot are sorted according to node addresses. The address of the last node serviced in the previous superframe is recorded, so that the allocations are assigned beginning from the next higher address. (Service policy in which nodes are served in a round-robin fashion and allowed to transmit at most one packet at a time is known as one-limited policy [11, 12]; it offers best performance at high traffic loads and ensures both short- and long-term fairness among the nodes.)

The allocations are announced in the assignment sub-frame which immediately follows the beacon. This packet is sent in the assignment sub-frame after the beacon, in the superframe at hop 2. (The allocation packet is shown in white, since it is received, rather than transmitted, by the current node.) The node then transmits its data packet to the designated receiver in that same superframe.

Allocation includes as many requests as can fit into one superframe, given that each node is granted transmission of at most one packet; requests that cannot fit in the current superframe are deferred to the next one(s). Appropriate announcements are made during the assignment sub-frame which immediately follows the beacon. The announcement also includes the channel which the coordinator would like to be sensed, but the node can choose to ignore that and perform the selection itself.

Upon transmitting the packet, the node has to perform sensing duty for k_s subsequent superframes, where k_s is the tax coefficient, before requesting to transmit another packet, as shown in Fig. 6.2. Sensing is performed by switching to the selected channel and listening to it for some time to decide whether there is a primary user activity. It may be done through energy detection, carrier detection, or feature identification, with an increasing accuracy but also with an increasing detection time [1].

Nodes that are currently engaged in sensing on account of an earlier transmission cannot request bandwidth again until they sense k_s primary channels and report the results of sensing to the coordinator.

Since sensing involves the overhead of switching channels back and forth, it is most efficient if performed throughout the entire data sub-frame; therefore the tax coefficient p will denote the number of sub-frames to spend in sensing. In this manner, each node given bandwidth to transmit actually pays for it by contributing to sensing. During the control sub-frame, the nodes that did sensing send the results back to the coordinator, which then updates the channel map and decides on the next working channel.

All nodes, regarding of whether they are currently doing the sensing duty or not, must listen to the beacon of the next superframe and subsequent assignment sub-frame. The reasoning behind this is simple: if a node that is currently sensing learns from the beacon that it is to receive a packet, it suspends sensing during that superframe, receives the packet, and resumes sensing after the next beacon frame. (Suspension may again be needed if another packet is to be received.) In theory a node could interrupt its sensing to switch back to the working channel, receive a packet, and then go back to finish sensing, the overhead of channel switching makes this prohibitively expensive, which is why we have adopted the simpler approach in which sensing is preempted by reception.

Transmission need not be suspended because of reception, as the node only has to switch its radio from one mode to another within the same superframe.

Packets that arrive during the transmission of an earlier packet and/or sensing are queued in the node buffer but not transmitted; bandwidth requests are prohibited until the node has spent at least p superframes in sensing. Sensing duty is thus discharged at the expense of extending the packet service cycle. Once the sensing is done, the node may immediately apply for bandwidth allocation in the next reservation sub-frame – if there are packets queued for transmission. This is the rationale for placing the control sub-frame before the reservation sub-frame; otherwise, a node would have to wait idle for an entire superframe before it could apply for bandwidth again.

6.3 Modeling the Protocol

Let us denote the time interval between two consecutive services of a given node, hereafter referred to as the piconet cycle, with C. Packet service cycle, denoted with Y, represents the time needed to service a single packet from the moment when the node applies for bandwidth. It consists of several components: waiting time for the beginning of round-robin packet service; packet service time (packet reception may occur in the same superframe); waiting time for the next beacon; potential reception of the packet; and spectrum sensing time.

From the viewpoint of queuing theory, interaction between transmission and sensing can be modeled as 1-limited M/G/1 system with vacations, in which packet transmission corresponds to the service period, while everything else – the sensing process, waiting for the transmission after requesting bandwidth from the coordinator, synchronization with the beacon, and potential reception of packet – comprises the total vacation period. These interactions are schematically depicted in Fig. 6.4 for the case with and without the preemption of the sensing process.

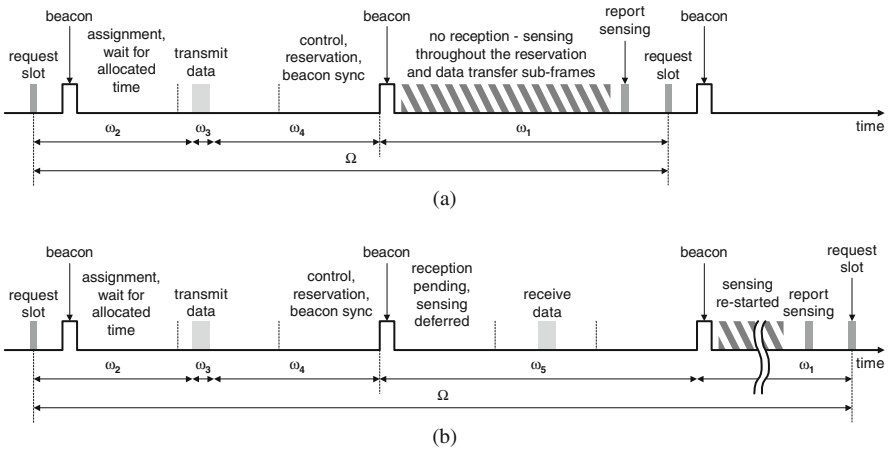

Fig. 6.4 Timing of node operation and distribution of arrivals during a service cycle. (**a**) Case without the preemption of sensing process; (**b**) Case with the preemption of sensing process

We assume that time is slotted and the total superframe length is s_f basic slots, while the packet size is constant and equal to k_d basic slots. Every data packet will be acknowledged immediately after the transmission, and the acknowledgment packet takes exactly one basic slot. Let the probability generating function (PGF) for the packet size with fixed size acknowledgment be $b(z) = z^{k_d+1}$ with a mean value of $\overline{b} = k_d + 1$. The Laplace–Stieltjes transform (LST) of the packet time (including the acknowledgment) is obtained by replacing the variable z with e^{-s}, i.e., $b^*(s) = \mathrm{e}^{-s(k_d+1)}$. Packets arrive to a node according to a Poisson process with the arrival rate of λ, so that the offered load to the node transmission interface is $\rho = \lambda \overline{Y}$. Nodes are assumed to have buffers of infinite capacity.

Vacation due to sensing activity – Each node has to perform k_s sensing events within the next superframe or several of them (if the node buffer is empty when sensing starts). From the aspect of queuing theory, this is a system with multiple vacations where the basic vacation duration is equal to one superframe. The PGF for the basic time spent in sensing is $V(z) = z^{s_f}$, with a mean value of $\overline{V} = s_f$, while the LST of a single vacation (sensing) period is $V^*(s) = \mathrm{e}^{-s_f s}$.

According to [12], the number of packet arrivals to the node during a single vacation period has the PGF of $\omega_1(z) = V^*(\lambda - \lambda z) = \sum_{k=0}^{\infty} f_k z^k$, and the probability of zero packet arrivals is $f_0 = V^*(\lambda)$.

Vacation due to waiting for round robin service – A node has to wait until all nodes with addresses lower than its own that have packets have been served. Assuming the CPAN has M nodes, the LST for the cycle time is $C^*(s) = ((1-\rho) + \rho S^*(s))^M$, where $S^*(s)$ is defined below. Then, the mean duration of the CPAN cycle is $\overline{C} = -C^{*'}(0) = -\left.\frac{dC^*(s)}{ds}\right|_{s=0} = \rho M \overline{S}$.

In terms of renewal theory [13], the time between the node request and (random) beginning of the service within the cycle is denoted as 'elapsed' or backward recurrence time in the discrete-time renewal process, where the distribution of the renewal interval is given by the cycle time C. Namely, the target node observes a cycle which starts with the node being served immediately after the beacon in the frame following its request for the bandwidth. Backward recurrence time will be denoted as C_- and its LST is $C_-^*(s) = \frac{1-C^*(s)}{s\overline{C}}$.

The number of packet arrivals while waiting for the round-robin service has the PGF of $\omega_2(z) = C_-^*(\lambda - \lambda z)$.

Duration of service period – Since only one packet can be transmitted in each service cycle, the PGF for the service time is $S(z) = b(z)$. The LST of the duration of node service period is $S^*(s) = b(e^{-s}) = b^*(s)$, and its mean value is $\overline{S} = \overline{b}$. Finally, the number of packet arrivals to the node during the transmission time has the PGF of $\omega_3(z) = S^*(\lambda - \lambda z)$.

Vacation due to synchronization – After packet transmission, the node needs to wait for the next control sub-frame in order to report sensing results to the coordinator. This waiting time presents 'residual' or forward recurrence time in the renewal period presented by the superframe. Its LST has the form $R_-^*(s) = \left(1 - e^{-s_f s}\right)/(s_f s)$, and the number of packet arrivals to the node buffer during that time has the PGF of $\omega_4(z) = R_-^*(\lambda - \lambda z)$.

Effect of packet reception – To model the impact of packet reception, we need the probability distribution of the time interval between transmission and reception by the given node. We will look at the piconet cycle started by the transmission by the target node $i \in 1 \ldots M$, where M is the number of nodes in the piconet. Reception by the target node will be triggered by some other node j, where j is between $i+1$ and $(i+M-1)$ mod M and we assume that the node address is located uniformly in that range.

Given that packet size is k_d slots and one slot is needed for acknowledgment, the PGF for the number of slots between transmission and reception by the node i is

$$\Theta(z) = \sum_{k=1}^{M-1} \frac{((1-\rho)+\rho S(z))^k}{M-1} = \sum_{i=1}^{(M-1)(k_d+1)} \theta_i z^i \tag{6.1}$$

and the probability that the node will transmit and receive in the same superframe is $P_\theta = P(\Theta < s_f - \Delta) = \sum_{i=1}^{s_f-\Delta} \theta_i$, where Δ represents the portion of the superframe dedicated to the reporting of sensing results and bandwidth reservation. The PGF for the number of packet arrivals during the superframe in which the node is engaged in reception is $\omega_5(z) = \mathrm{e}^{-s_f(\lambda-\lambda z)}$.

6.4 Packet Service Cycle and Access Delay

A packet service cycle begins when the node applies for bandwidth and ends when the node returns from sensing associated with the packet which was transmitted in this cycle. Each packet needs a total service time with a LST of $Y^*(s) = S^*(s)C^*(s)R^*(s)\left(P_\theta + (1-P_\theta)e^{-s_f s}\right)V^*(s)$, and an average value of $\overline{Y} = \overline{S} + \overline{C} + \overline{R} + (1-P_\theta)s_f + \overline{V}$. The offered load then becomes $\rho = \lambda\overline{Y}$, instead of $\rho' = \lambda\overline{S}$ as is the case for exhaustive service. As both cycle time and probability of reception in the same superframe are functions of offered load, the equation for $\overline{Y}$ can actually be solved for ρ. The PGF for the number of packet arrivals during the packet service cycle is $\Omega(z) = \omega_1(z)\omega_2(z)\omega_3(z)\omega_4(z)\left(P_\theta + (1-P_\theta)\omega_5(z)\right)$.

Let us now consider the node packet queue length at the moments of end of packet service cycle and at the end of the node's vacation. The probability that there are k packets in the queue after packet's service cycle is denoted with π_k, and the PGF for the queue length after a packet service cycle is denoted with $\Pi(z) = \sum_{k=0}^{\infty} \pi_k z^k$. Probability that there are k packets in device queue at the end of a single vacation is denoted with q_k, while the PGF for the queue length after the sensing period is denoted with $Q(z) = \sum_{k=0}^{\infty} q_k z^k$. Then, the state transition equations for these two kinds of Markov points are

$$\begin{aligned} q_k &= (q_0 + \pi_0) f_k && k \geq 0 \\ \pi_k &= \sum_{j=1}^{k+1} (q_j + \pi_j) a_{k-j+1} && k \geq 0 \end{aligned} \tag{6.2}$$

subject to condition $\sum_{k=0}^{\infty} q_k + \sum_{k=0}^{\infty} \pi_k = 1$. The PGFs $\Pi(z)$ and $Q(z)$ then become

$$\begin{aligned} \Pi(z) &= \frac{1-\lambda\overline{Y}}{1-\lambda\overline{Y}+\lambda\overline{V}} \cdot \frac{Y^*(\lambda-\lambda z)(1-V^*(\lambda-\lambda z))}{Y^*(\lambda-\lambda z)-z} \\ Q(z) &= \frac{1-\lambda\overline{Y}}{1-\lambda\overline{Y}+\lambda\overline{V}} V^*(\lambda-\lambda z) \end{aligned} \tag{6.3}$$

Knowing $Q(z)$, we can find $q_0 = \frac{f_0(1-\rho)}{1-\rho+\lambda\overline{V}}$. Moreover, we are able to find the probability distribution of the entire node inactive period (which occurs when the node finds an empty buffer after sensing in the current superframe) as $I(z) = V(z)(1-q_0)\sum_{k=0}^{\infty}(V(z)q_0)^k$, with an average value of $\overline{I} = \overline{V}/(1-q_0)$.

The PGF for the number of packets in the device queue immediately after a packet departure is

$$\Pi_d(z) = \frac{\Pi(z)-\pi_0+Q(z)-q_0}{(1-\pi_0-q_0)z}\,\omega_2(z)\omega_3(z) \tag{6.4}$$

and the average number of packets left after a packet departure is $\overline{L} = \Pi_d'(1) = \overline{\omega_2} + \overline{\omega_3} - \frac{1}{2} + \frac{\omega_1^{(2)}}{2\overline{\alpha}} + \frac{\Omega^{(2)}}{2(1-\rho)} - \frac{\rho}{2(1-\rho)}$, where $\omega_1^{(2)}$ denotes the second moment of the number of packet arrivals during the vacation time and $\Omega^{(2)}$ denotes the second moment of the number of packet arrivals during the packet service cycle.

Probability distribution of the waiting time in the node buffer can be found from the observation that, under the FIFO serving discipline, the number of packets left after a packet departure is equal to the number of packets which have arrived to the queue while the target packet was in the system. Therefore, $\Pi_d(z) = T_a^*(\lambda-\lambda z) = W^*(\lambda-\lambda z)Y^*(\lambda-\lambda z)$.

6.5 Model of the Sensing Process

Upon completing their packet transmissions, ordinary nodes revert to sensing of k_s channels out of N working channels in the RF band. Given the results of the previous section, let us denote the probability that a node is available for sensing as $P_{\text{sec}} = k_s\overline{V}/\left(\overline{Y}-\overline{V}+\overline{I}\right)$. Then, the number of secondary nodes X_{sec} available for sensing is a random variable; under constant packet arrival rate (per node) of λ and piconet size M, this number has a binomial distribution with the PGF of

$$X_{\text{sec}}(y) = \sum_{j=0}^{M} \binom{M}{j} P_{\text{sec}}^j (1-P_{\text{sec}})^{M-j} y^j \tag{6.5}$$

with the average value of $\overline{X_{\text{sec}}} = P_{\text{sec}}M$. Note that we use variable y in the PGF to carry mass probabilities related to the number of sensors active at any given time.

Since sensing is performed in discrete intervals, and the number of nodes available for sensing is typically lower than the number of channels, $X_{\text{sec}} < N$, the information available to the coordinator is only partially correct at any given time. The magnitude of the error (i.e., the mean number of channels with incorrect information) and the delay in detecting changes in channel status will determine the success rate of CPAN transmissions and, ultimately, its QoS.

Without loss of generality, we may also assume that each of the N working channels is used by a distinct primary user or source. For simplicity, we will assume that active and idle times on each channel follow the probability distributions with cumulative density functions $T_{a,r}(x)$ and $T_{i,r}(x)$, and mean values of $\overline{T_{a,r}}$ and $\overline{T_{i,r}}$, respectively. The mean value of real cycle time will be denoted as $\overline{T_{\text{cyc},r}} = \overline{T_{a,r}} + \overline{T_{i,r}}$. For clarity, we will denote relevant variables in the active and idle (free) periods of the channel state, with subscripts a and i, respectively, while the subscripts r and o will denote real and observed values of respective network parameters.

Sensing is performed in a frequency hopping manner with the sensing period regulated by the occupancy of the node's data queue. As long as the node buffer is empty, the period between consecutive sensing actions is equal to the superframe duration s_f. As explained above, if there is a packet in the node buffer at any time during sensing, the node will accelerate sensing to one sensing per basic slot, so that the remaining sensing activity can be completed within the current superframe. Therefore, the sensing period is a random variable with the PGF of

$$T_s(z) = (1-\pi_0)z + \pi_0 \left((1-q_0) \sum_{j=1}^{k_s-1} q_0^{j-1} \left(\frac{j}{k_s} z^{s_f} + \frac{k_s - j}{k_s} z \right) + q_0^{k_s} z^{s_f} \right) \quad (6.6)$$

where the variable z carries the mass probabilities of time periods between successive sensing events.

Assuming that $T_s \ll \overline{T_{a,r}}, \overline{T_{i,r}}$, the probability distributions of active and inactive times of primary users may be considered discrete, and their state changes can occur at the boundaries of the sensing period T_s. Let us denote the PGFs for active and idle times of primary user activity as $T_{a,r}(z) = \sum_{k=0}^{\infty} p_a(k) z^k$ and $T_{i,r}(z) = \sum_{k=0}^{\infty} p_i(k) z^k$, where the variable z corresponds to the sensing period T_s. For example, if $T_{a,r}$ and $T_{i,r}$ are geometrically distributed with parameters α and β respectively, then $p_a(k) = \alpha(1-\alpha)^{k-1}$ and $p_i(k) = \beta(1-\beta)^{k-1}$.

At the beginning of the superframe, CPAN coordinator announces that X_{sec} nodes will sense primary channels, some of which are marked as idle in the channel map while others are marked as active. Due to random selection of channels to sense and random allocation of these channels to sensing nodes, a given sensing node need not be tied to sensing only idle or only active channels. Since the average interval between successive sensing events depends on the ratio of the number of sensing nodes and the number of channels, the sensing intervals for idle and active channels will be equal, as will be the delays in detecting the beginning and end of channel activity.

Let the mean observed durations of active and inactive period be $\overline{T_{i,o}}$ and $\overline{T_{a,o}}$, respectively. Then, the probability that a channel is idle (as observed via the channel map) is $p_{i,o} = \frac{\overline{T_{i,o}}}{\overline{T_{a,o}}+\overline{T_{i,o}}}$, while the probability that a channel is active is $p_{a,o} = 1 - p_{i,o}$. The mean observed numbers of idle and active channels are $\overline{N_{i,o}} = p_{i,o}N$ and $\overline{N_{a,o}} = p_{a,o}N = N - \overline{N_{i,o}}$, respectively. On the other hand, the probability that a channel is actually idle is $p_{i,r} = \frac{\overline{T_{i,r}}}{\overline{T_{a,r}}+\overline{T_{i,r}}} \neq p_{i,o}$, and by the same token $p_{a,r} \neq p_{a,o}$.

The choice of channels to be sensed is made randomly, but no channel is sensed by more than one sensing node as long as the number of sensors is smaller than the number of channels.

Then, the PGF for the single-channel sensing rate becomes

$$P_w(y) = \sum_{j=0}^{M} \binom{X}{j} P_{\text{sec}}^{j}(1 - P_{\text{sec}})^{M-j} y^{\frac{j}{N}} \tag{6.7}$$

when $X_{\text{sec}} < N$, and $P_w(y) = y$, otherwise. This polynomial does not qualify as a PGF, since the exponents of y are not integers. However, it satisfies the condition that $P_w(1) = 1$ and its mean value is finite, $\overline{P_w} = P'_w(1)$, and therefore it does represent a probability distribution.

The time between two consecutive sensing events on the same channel is a random variable which depends on the number of sensors and on the sensing period of a particular sensor. It has geometric distribution with respect to the sensing period and binomial distribution with respect to the number of sensors available for sensing, i.e.,

$$\begin{aligned} H(y,z) &= \sum_{j=0}^{M} \frac{T_s(z)\,j}{(1 - T_s(z)(1 - \frac{j}{N}))} y^{\frac{j}{N}} \cdot \binom{M}{j} P_{\text{sec}}^{j}(1 - P_{\text{sec}})^{M-j}, \; X_{\text{sec}} < N \\ H(y,z) &= yT_s(z) \qquad\qquad X_{\text{sec}} \geq N \end{aligned} \tag{6.8}$$

Using the results of renewal theory [13] it is possible to calculate probability distribution between the change of channel state and next sensing event. The sensing process for a single channel may be considered as a discrete-time renewal process where sensing events correspond to renewal points, while the renewal time corresponds to the period between two consecutive sensing events. In terms of renewal theory, the time between the channel state change and the next sensing event is denoted as the residual life(time) or forward recurrence time; Then, the probability generating function for the residual sensing time can be derived as

$$R(y,z) = \sum_{j=0}^{M} \sum_{k=0}^{\infty} R_{j,k} z^k y^{\frac{j}{N}} = \frac{1 - H(y,z)}{\overline{h}(1 - z)} \tag{6.9}$$

and the mean value of the residual sensing time is

$$\overline{R} = \frac{\lim\limits_{z\to 1}\lim\limits_{y\to 1}\dfrac{\partial^2 H(y,z)}{\partial z^2}}{2\lim\limits_{z\to 1}\lim\limits_{y\to 1}\dfrac{\partial H(y,z)}{\partial z}} \tag{6.10}$$

From the above system of equations we can find the values of $p_{i,o}$, $p_{i,a}$, $P_{w,i}$, $P_{w,a}$, and $\overline{R}$. The average delays in detecting inactivity and activity of the channel are $(1 - p_{s,i})\overline{R}$ and $(1 - p_{s,a})\overline{R}$, respectively. Given that the primary source is idle or active with the probabilities $p_{i,r} = \frac{\overline{T_{i,r}}}{\overline{T_{a,r}}+\overline{T_{i,r}}}$ and $p_{a,r} = 1 - p_{i,r}$, respectively, the number of channels with obsolete information will be $E_a = a_1 p_{a,r} N$, for active channels, and $E_i = b_1(1 - p_{a,r})N$, for idle ones.

We note that skipping an entire active or inactive period will also affect the duration of incorrect information about channel state, which will now differ from the residual sensing time. More details about the impact of this can be found in [8].

6.6 Performance of the Original Protocol

In order to evaluate the performance of the proposed scheme we had to evaluate the performance of transmission scheduling as well as that of channel sensing. Our evaluation environment used the following basic assumptions:

- Time is partitioned into basic time slots of equal duration; to ensure generality, all calculations are done in units of time slots.
- There are 30 primary channels, each with an independent ON-OFF source that has a negative exponential distribution of active and inactive periods. The mean activity period is 1000 unit time slots, with the mean duty cycle of 1/3.
- Each superframe has a duration of 100 unit time slots; the duration of the data/sensing sub-frame is set to 85 time slots.
- The CPAN consists of a variable number of identical nodes and a dedicated coordinator. The coordinator neither generates nor receives any data traffic.
- Each node generates packets at a variable rate according to Poisson distribution. The destinations are uniformly distributed over all other nodes. Packet duration was set to 10 unit time slots, with an optional acknowledgment.
- Each node has a buffer with 20 packets capacity; packets that arrive to a full buffer are simply dropped.
- Each node is allowed to request a single packet transmission slot from the coordinator; the requests are serviced in the round-robin fashion. The allocation announcement includes the number of the channel that the coordinator would like to be sensed.
- Once it has transmitted its packet, the node performs sensing on a certain number of channels. We have assumed that the sensing of a single channel, including the

channel switching overhead, lasts for 8 unit time slots (which is rather conservative). The node can therefore sense up to 10 channels in a single superframe; for simplicity, we assume that sensing is perfect and there is no discrepancy between sensing results obtained by different nodes. (This will be a topic for future research, since the focus of this chapter is the tradeoff between data transmission and sensing.)

We have then solved the system of equations outlined above using Maple 11 by Maplesoft, Inc. [14]. The results are as follows.

To evaluate the performance of the transmission-tax based MAC protocol, we have performed two experiments, first by fixing the number of CPAN nodes to 15 and varying the packet arrival rate between 0.0005 and 0.003 packets per unit time slot per node and second by fixing the packet arrival rate to 0.0015 packets per unit time slot per node and varying the number of CPAN nodes between 15 and 40; in both cases, the other variable parameter was the tax coefficient, i.e., the number of superframes to be spent in sensing for each packet transmitted.

Performance of data transmission in the CPAN, as indicated by mean packet access delay, offered load, and mean blocking probability at the device buffer, is illustrated through diagrams in Fig. 6.5. As could be expected, the CPAN enters saturation at higher packet arrival rates and/or higher values of the tax coefficient, as both lead to more sensing. However, when the nodes spend too much time in sensing, they do not transmit data as often, their input buffers overflow and too many packets are dropped; hence the blocking probability exhibits a sharp increase. As a result, the offered load, increases in an almost linear fashion when the tax coefficient is 1, but begins to flatten out at higher tax rates; for tax coefficient of 5, offered load cannot exceed 0.26 due to extensive sensing. Note that the offered load was calculated with reference to the duration of the data/sense sub-frame, i.e., 85 unit time slots, rather than relative to the entire superframe duration of 100 unit time slots.

The sensing performance, expressed as mean number of nodes reporting sensing results per superframe, mean number of sensing reports received per superframe, mean number of channels for which the information in the channel map is incorrect, and mean delay in detecting the beginning or end of primary user activity, is shown in Fig. 6.6. As can be seen, the onset in saturation is also reflected in distinct flattening of the number of reporting nodes per superframe in Fig. 6.6a, as well as in an increase of sensing error, Fig. 6.6c. Interestingly enough, another measure of sensing accuracy – the detection delay – flattens out in the saturation regime. Note that the number of reports received does include duplicate reports; as mentioned above, we assume that sensing is perfect, and leave the issue of reconciling different sensing results for future work.

The number of sensing nodes and the number of sensing reports increase with both the tax coefficient and the number of CPAN nodes. Sensing accuracy, however, does not improve in the same manner: the sensing error decreases linearly with the number of nodes, but shows a floor when the tax coefficient increases, even though the number of nodes exceeds the number of channels in part of the observed range.

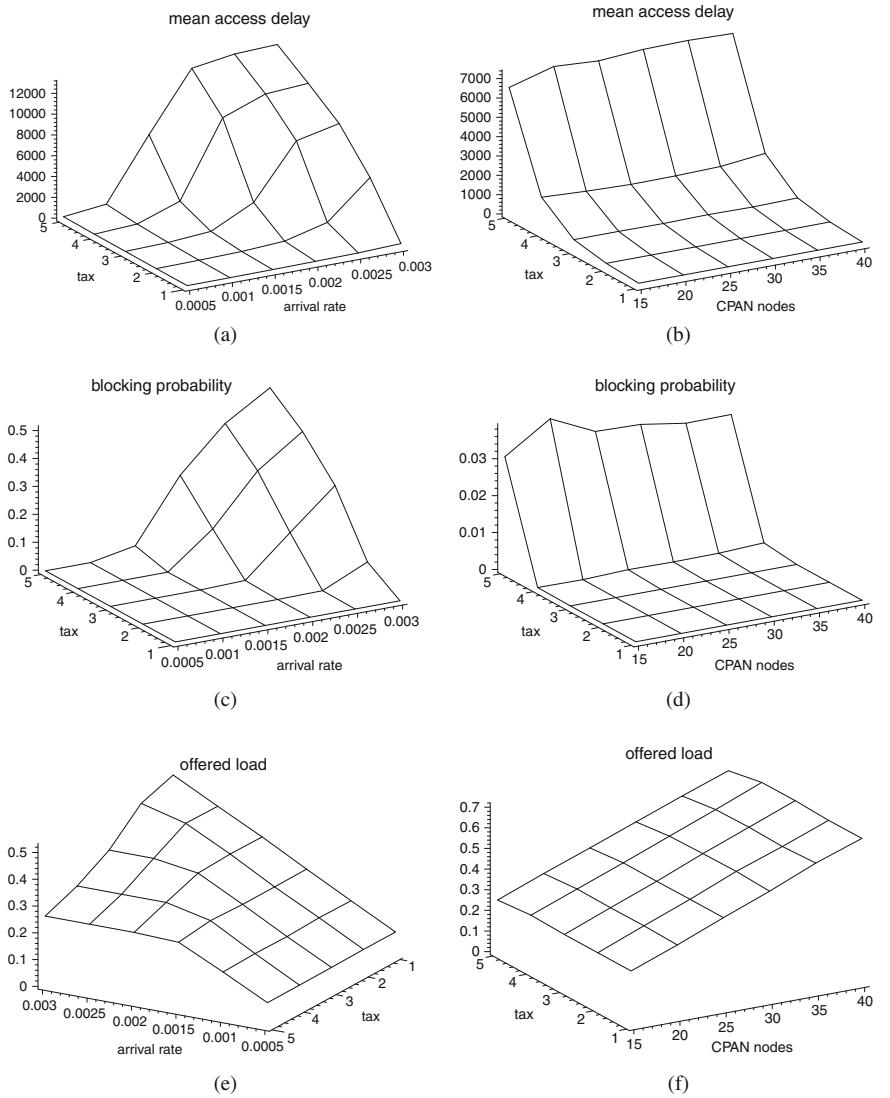

Fig. 6.5 Original transmission tax protocol: data communication performance. On the *left*, variable packet arrival rate and tax coefficient; on the *right*, variable number of CPAN nodes and tax coefficient. (**a**) Mean packet access delay; (**b**) Mean packet access delay; (**c**) Mean blocking probability at the device buffer; (**d**) Mean blocking probability at the device buffer; (**e**) Offered load; (**f**) Offered load (note the different orientation of the plot)

This is the consequence of primary user activity following a negative exponential distribution.

Finally, to evaluate the impact of sensing on the operation of the CPAN, we have also measured the probability that a channel which is considered to be free at the

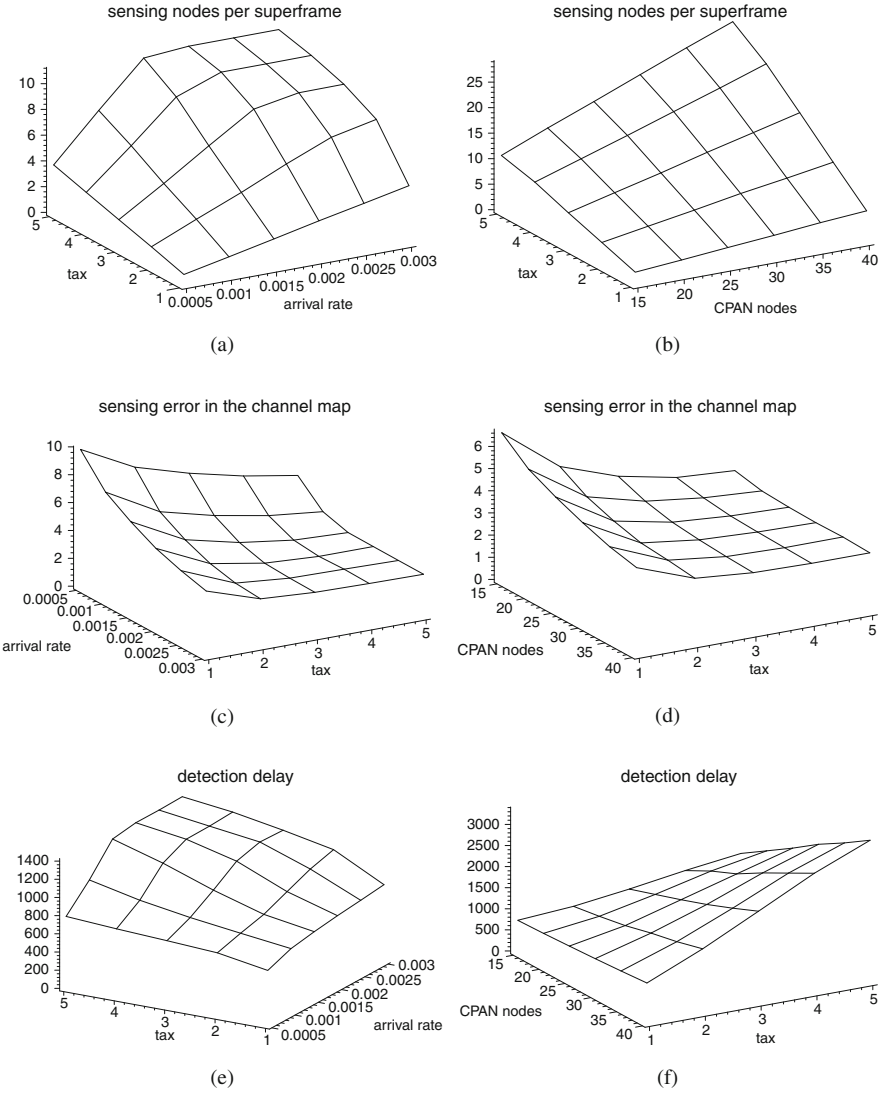

Fig. 6.6 Original transmission tax protocol: sensing performance. On the left, variable packet arrival rate and tax coefficient; on the right, variable number of CPAN nodes and tax coefficient. (**a**) Mean number of reporting nodes per superframe; (**b**) Mean number of reporting nodes per superframe; (**c**) Mean number of incorrect entries in the channel map; (**d**) Mean number of incorrect entries in the channel map; (**e**) Mean detection delay for primary user activity; (**f**) Mean detection delay for primary user activity

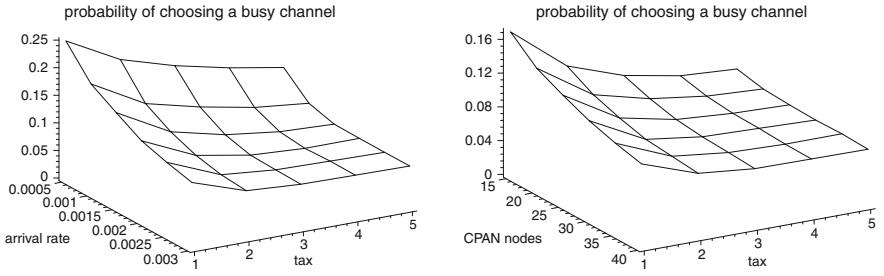

Fig. 6.7 CPAN performance under original transmission tax protocol: probability of selecting a busy channel for the next hop. (**a**) Under variable packet arrival rate and tax coefficient; (**b**) Under variable number of primary channels and tax coefficient

end of the control sub-frame – i.e., at the time when the coordinator checks the channel map in order to make the decision about the next hop for the entire CPAN – is actually busy; the corresponding diagrams are shown in Fig. 6.7. As can be seen, this probability drops when the tax coefficient increases; it is also influenced by the number of nodes in the CPAN and mean arrival rate, as could be expected.

6.7 Can Channel Ordering Improve Sensing Accuracy?

One possible area of improvement appears to be the selection of channels to be sensed. The simplest solution is to allow for random selection by the nodes themselves; this is how the data shown in Figs. 6.5, 6.6, and 6.7 have been obtained. Intuitively, sensing accuracy should be improved if preference is given to channels for which the information in the channel map is the least recent. By focusing on the least recently sensed channels, the mean age of the sensing information could be reduced, with the ensuing improvement in the accuracy of the channel map.

Since the coordinator records the sensing reports in the channel map, it is easy to modify the channel map to include the information about the actual time when the sensing report was received. Moreover, appropriate additions were made to the design of ordinary nodes so that they can also keep track of the sensing time. In one experiment, the coordinator instructed the nodes to begin sensing from the channels with least recent information. Since the packet format includes provisions for only one channel (the coordinator does not know for sure how many channels will the node be able to sense in one superframe), the remaining channels were assigned at random by the node itself. In the second experiment, the nodes themselves performed sensing on the channels for which their local information was least recent. The sensing performance obtained in these two experiments, referred to as centralized and distributed solution, respectively, are shown in Figs. 6.8 and 6.9. As can be seen, local selection (the second set of diagrams) gives somewhat better sensing accuracy, although the difference is not too big.

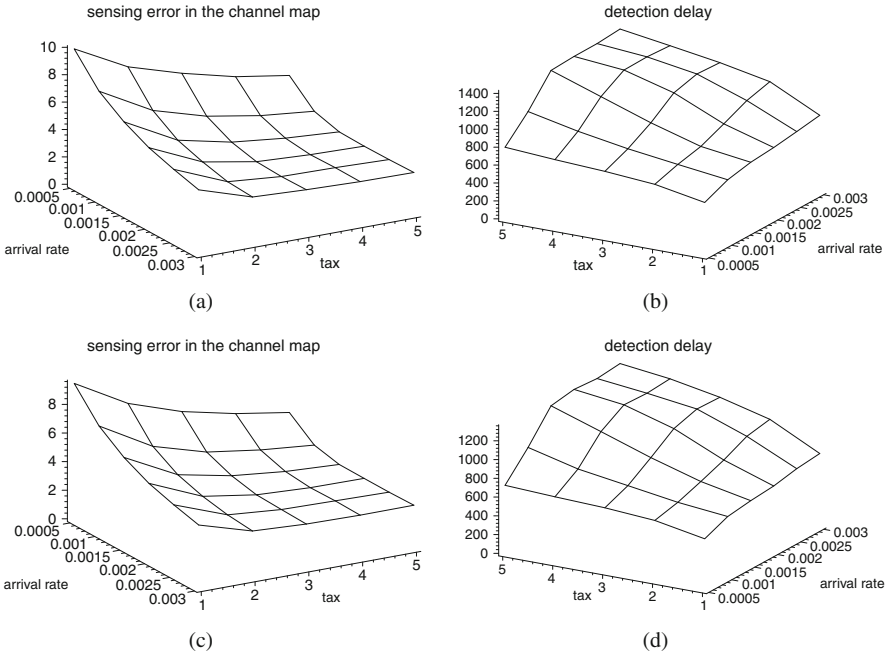

Fig. 6.8 Sensing performance of the protocol modified to account for least recently sensed channels, part I: centralized selection of channels to sense. (**a**) Mean number of incorrect entries in the channel map; (**b**) Mean detection delay for primary user activity; (**c**) Mean number of incorrect entries in the channel map; (**d**) Mean detection delay for primary user activity

Fortunately, the improvement in sensing accuracy does not come at the expense of data transmission performance, shown in Fig. 6.10 for the case of local selection of channels to be sensed; as can be seen, mean access delay and blocking probability are virtually unaffected by this modification.

6.8 Adapting the Transmission Tax

One of the problems with the transmission tax is that the actual amount of sensing information is highly dependent on the data traffic. Namely, when several nodes apply for bandwidth, we may expect abundant sensing information in the next superframes – with a lot of overlap; but when only one node applies, or none at all, there will be a dearth of sensing reports in the next few superframes. This imbalance might be remedied by making the tax coefficient vary in inverse proportion to data traffic intensity: it can be low when there are many transmission requests, but must be high when there are only few of them.

To this end, we have built a simulator of the protocol, using the object-oriented Petri net-based simulation engine Artifex [15], and included adaptive calculation of the tax coefficient using the algorithm below. Namely, in each superframe, the

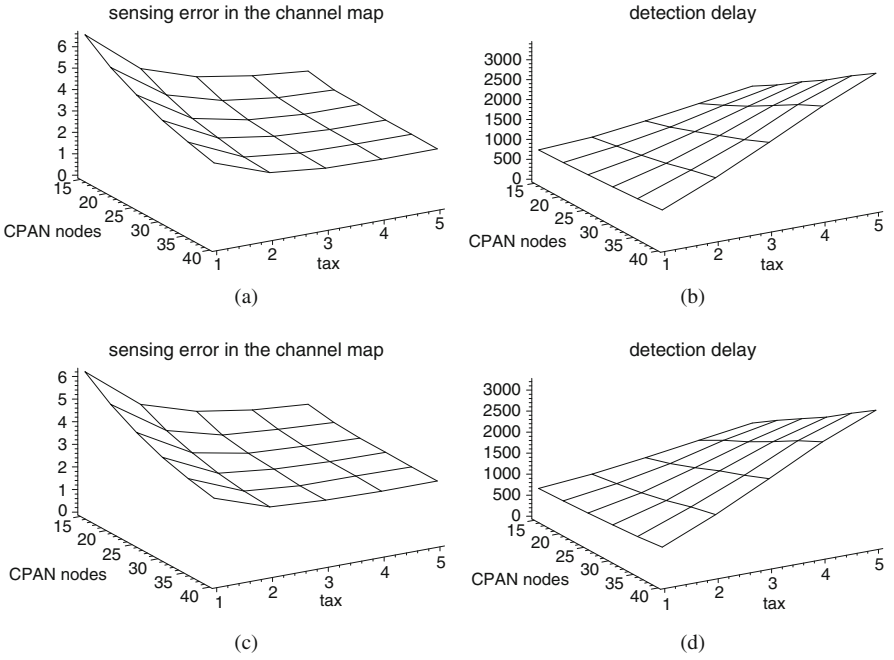

Fig. 6.9 Sensing performance of the protocol modified to account for least recently sensed channels, part II: local selection of channels to sense. (**a**) Mean number of incorrect entries in the channel map; (**b**) Mean detection delay for primary user activity; (**c**) Mean number of incorrect entries in the channel map; (**d**) Mean detection delay for primary user activity

coordinator updates an exponential moving average (EWMA) of the number of distinct channels sensed per superframe, denoted with S; this number is compared to the total number of channels N and the new value of the tax coefficient is calculated on the basis of this comparison. The updated value of the tax coefficient is then broadcast to all the nodes in the beacon frame; nodes that have to perform sensing will use this value throughout their sensing duty, even though it may go up or down in subsequent superframes.

Algorithm 1 : Adaptive calculation of the tax coefficient.

Input: number of sensing reports in the last superframe s;
number of incoming transmission requests r;
maximum number of channels that can be sensed in a superframe σ;
smoothing coefficient α
Result: tax coefficient t

1 calculate $S(i+1) = \alpha * S(i) + (1-\alpha) * s$;
2 calculate raw tax coefficient as $\tau = (N/r) * \sigma$;
3 **if** $S(i+1) > M/2$ **then** $t = \tau$;
4 **else if** $S(i+1) > M/3$ **then** $t = 1.0 + \tau$;
5 **else if** $S(i+1) > M/4$ **then** $t = 2.0 + \tau$;
6 **else** $t = 3.0 + \tau$;

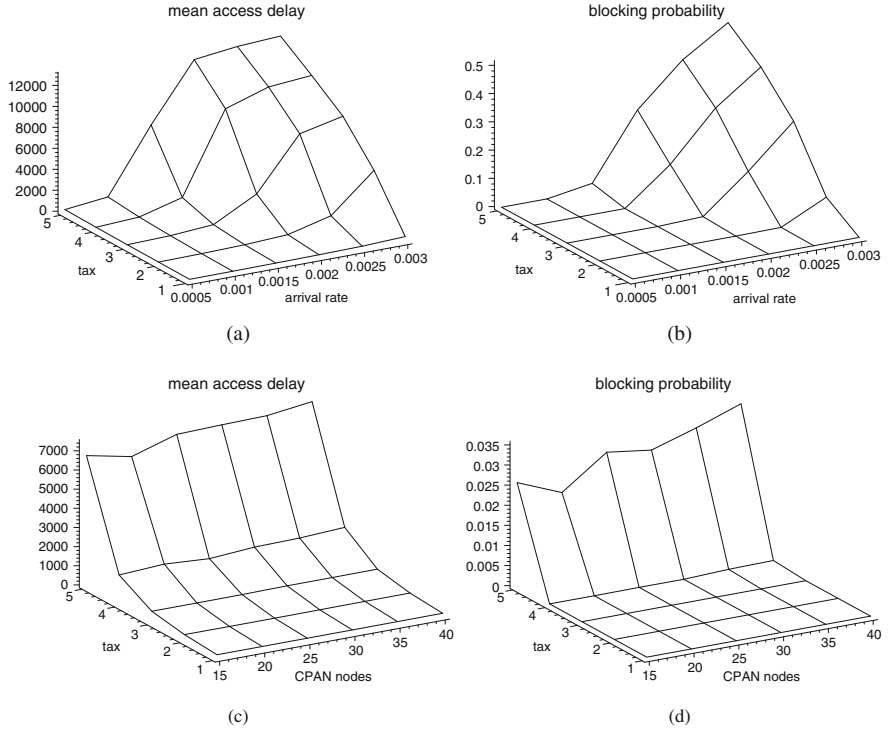

Fig. 6.10 Protocol modified to include local selection of the channel to sense: data communication performance. *Top row*: variable packet arrival rate and tax coefficient; *bottom row*: variable number of CPAN nodes and tax coefficient. (**a**) Mean packet access delay; (**b**) Mean blocking probability at the device buffer; (**c**) Mean packet access delay; (**d**) Mean blocking probability at the device buffer

The results obtained with the adaptive algorithm are shown in Figs. 6.11 and 6.12, for data transmission and sensing performance, respectively. As can be seen, the improvement in data transmission performance is drastic: access delays are low and offered load increases almost linearly with the arrival rate, reaching the value of approx. 0.7 when the CPAN has 40 nodes. At the same time, the CPAN does not come close to saturation in the observed range of arrival rates – blocking probability does not exceed 10^{-4}, which is why it is not shown. Sensing performance is also improved, esp. the detection delay which stays below 900 unit time slots throughout the observed range of independent variables. In all the diagrams, solid lines correspond to the case without least-recently-sensed modification, while diamonds and asterisks correspond to the centralized and local least-recently-sensed channel selection, respectively; however, the differences are minuscule, even though the sensing error is lower under local selection of least-recently-sensed channels.

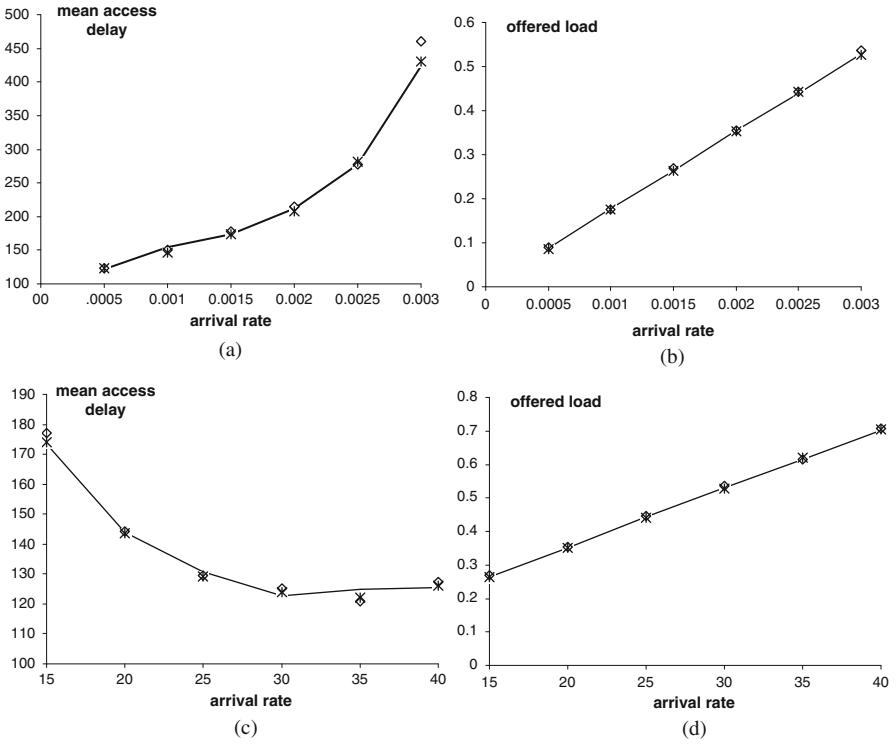

Fig. 6.11 Adaptive protocol: data transmission performance. (**a**) Mean access delay vs. packet arrival rate; (**b**) Offered load vs. packet arrival rate; (**c**) Mean access delay vs. number of CPAN nodes; (**d**) Offered load vs. number of CPAN nodes

6.9 Conclusion

We have presented one possible scheme of interaction between transmission and sensing in cognitive personal area networks and investigated its performance through analytical modeling and simulation. The scheme conforms to the 1-limited round robin service policy, where nodes can transmit only single packet they've had at the moment of applying for the bandwidth using the first-come, first-served policy. In addition, nodes need to perform sensing duty after each transmitted packet in order to control the sensing error. Reception is not penalized because it is associated with transmission, and because it may have to be performed at the expense of extending the sensing cycle.

We have modeled the effect of packet reception of the node which might preempt, but not reduce sensing activity. In this manner, total sensing time is not affected; instead, any reception actually contributes to the packet delay. The 1-limited policy is simple to implement and fair to all nodes. However, it suffers from the overhead associated with each transmitted packet, which limits the stable operation region.

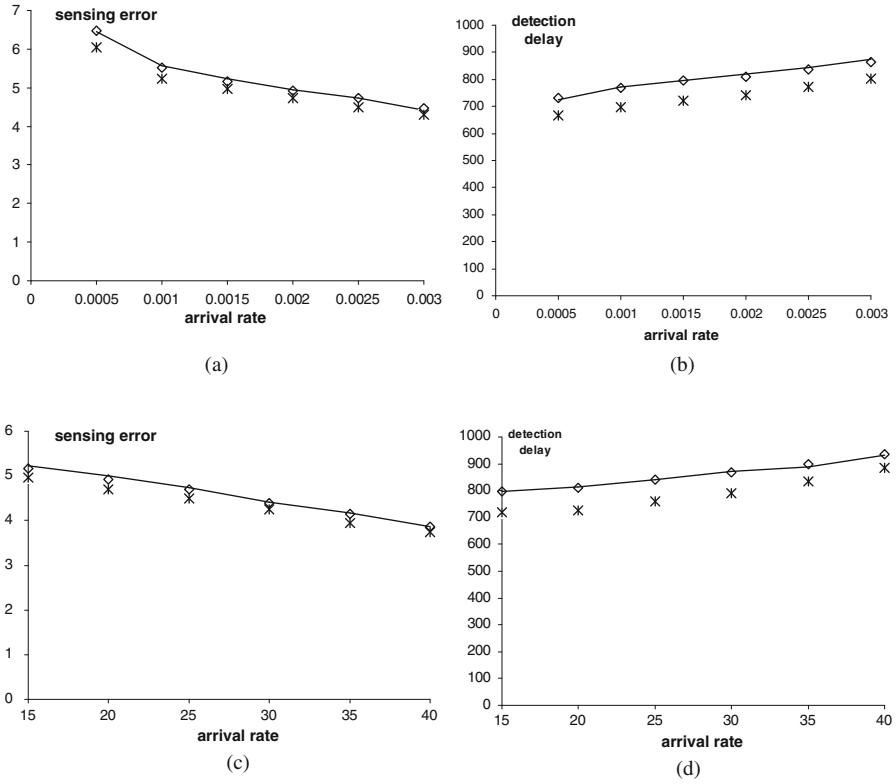

Fig. 6.12 Adaptive protocol: sensing performance. (**a**) Sensing error vs. packet arrival rate; (**b**) Detection delay vs. packet arrival rate; (**c**) Sensing error vs. number of CPAN nodes; (**d**) Detection delay vs. number of CPAN nodes

We have also integrated the sensing policy which controls the total sensing error with the packet transmission policy. Control policy limits the total error on all channels and calculates the necessary number of sensing events per each transmitted packet. Our results indicate that future refinement of the integrated sensing-for-transmission policy is needed in order to separately control the sensing error on active and idle channels.

Finally, we have shown that the performance of the MAC with respect to both data transmission and sensing is vastly improved if the tax coefficient is dynamically adapted to traffic variations, and that slight improvements in sensing accuracy may be obtained when the selection of channels to be sensed is performed locally by each node.

References

1. Ian F. Akyildiz, Won-Yeol Lee, Mehmet C. Vuran, and Shantidev Mohanty. NeXt generation/dynamic spectrum access/cognitive radio wireless networks: A survey. *Computer Networks*, 50:2127–2159, 2006.

2. Bluetooth SIG. *Core Specification of the Bluetooth System*. Version 2.0 + EDR, November 2004.
3. DARPA. The XG vision. Request for comments, January 2004.
4. Stefan Geirhofer, Lang Tong, and Brian M. Sadler. Cognitive medium access: A protocol for enhancing coexistence in WLAN bands. In *Proceedings Global Telecommunications Conference GLOBECOM'07*, Washington, DC, November 2007.
5. D. P. Heyman and M. J. Sobel. *Stochastic Models in Operations Research, Volume 1: Stochastic Processes and Operating Characteristics*. McGraw-Hill, New York, 1982.
6. IEEE. Wireless MAC and PHY specifications for high rate WPAN. IEEE Std 802.15.3, IEEE, New York, NY, 2003.
7. Paul K. Lee. Joint frequency hopping and adaptive spectrum exploitation. In *IEEE Military Communications Conference MILCOM2001*, volume 1, pages 566–570, October 2001.
8. Hanoch Levy, Moshe Sidi, and Onno J. Boxma. Dominance relations in polling systems. *Queueing Systems Theory and Applications*, 6(2):155–171, 1990.
9. Ying-Chang Liang, Yonghong Zeng, E.C.Y. Peh, and Anh Tuan Hoang. Sensing-throughput tradeoff for cognitive radio networks. *IEEE Transactions on Wireless Communications*, 7(4):1326–1337, 2008.
10. Maplesoft, Inc. *Maple 11*. Waterloo, ON, Canada, 2007.
11. Jelena Mišić and Vojislav B. Mišić. Performance of cooperative sensing at the MAC level: Error minimization through differential sensing. *IEEE Transactions on Vehicular Technology*, 58(5):2457–2470, 2009.
12. Jelena Mišić and Vojislav B. Mišić. Simple and efficient MAC for cognitive wireless personal area networks. In *Proceedings Global Telecommunications Conference GLOBECOM'09*, Honolulu, HI, November 2009.
13. RSoft Design. *Artifex v.4.4.2*. RSoft Design Group, San Jose, CA, 2003.
14. Hideaki Takagi. *Queueing Analysis*, volume 1: Vacation and Priority Systems. North-Holland, Amsterdam, The Netherlands, 1991.
15. Danijela Čabrić, Shridhar Mubaraq Mishra, Daniel Willkomm, Robert Brodersen, and Adam Wolisz. A cognitive radio approach for usage of virtual unlicensed spectrum. In *Proceedings of the 14th IST Mobile Wireless Communications Summit*, Dresden, Germany, June 2005.